Vacuum diffraction at finite spatio-temporal offset

Ricardo Oude Weernink, Felix Karbstein
Theoretisch-Physikalisches-Institut, Friedrich-Schiller-Universität Jena
Helmholtz Institute Jena

FRIEDRICH-SCHILLER-UNIVERSITÄT JENA — HELMHOLTZ Helmholtz-Institut Jena

1. Introduction

The classical Maxwell theory assumes vacua as being void. Within QED however this picture is expanded by non-linear effects related to virtual particle fluctuations, with the leading interaction describing the coupling of four photons. Typical experimental scenarios rely on pump-probe-type schemes.

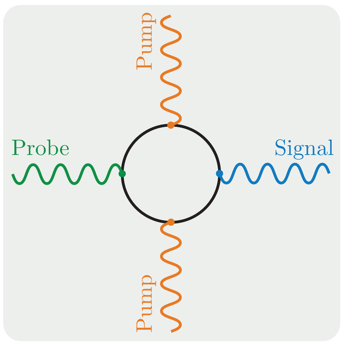

Formally we can study this process on the basis of the effective Heisenberg-Euler Lagrangian $\mathcal{L}_{\rm HE} = \mathcal{L}_{\rm MW} + \mathcal{L}_{\rm int}$, with classical Maxwell term $\mathcal{L}_{\rm MW} = -\frac{1}{4}F_{\mu\nu}F^{\mu\nu}$ and

$$\mathcal{L}_{\rm int} \simeq \frac{2\alpha^2}{45 m_e^4}\left[\left(F^{\mu\nu}F_{\mu\nu}\right)^2 + \frac{7}{4}\left({}^*F_{\mu\nu}F^{\mu\nu}\right)^2\right] .$$

The corresponding zero-to-single signal photon amplitude reads

$$S(\mathbf{k}) = \langle\gamma(\mathbf{k})| \int \mathrm{d}^4x\, f^{\mu\nu}(x)\frac{\partial\mathcal{L}_{\rm int}}{\partial F^{\mu\nu}}(x)|0\rangle ,$$

resulting in the differential number of signal photons via Fermi's golden rule

$$\mathrm{d}^3N(\mathbf{k}) = \frac{\mathrm{d}^3k}{(2\pi)^3}|S(\mathbf{k})|^2 .$$

A recent publication [1] studied the influence of beam curvature on optical signatures at SACLA laboratory; a thorough quantitative analysis seemed beneficial.

2. Pump-Probe-Setup

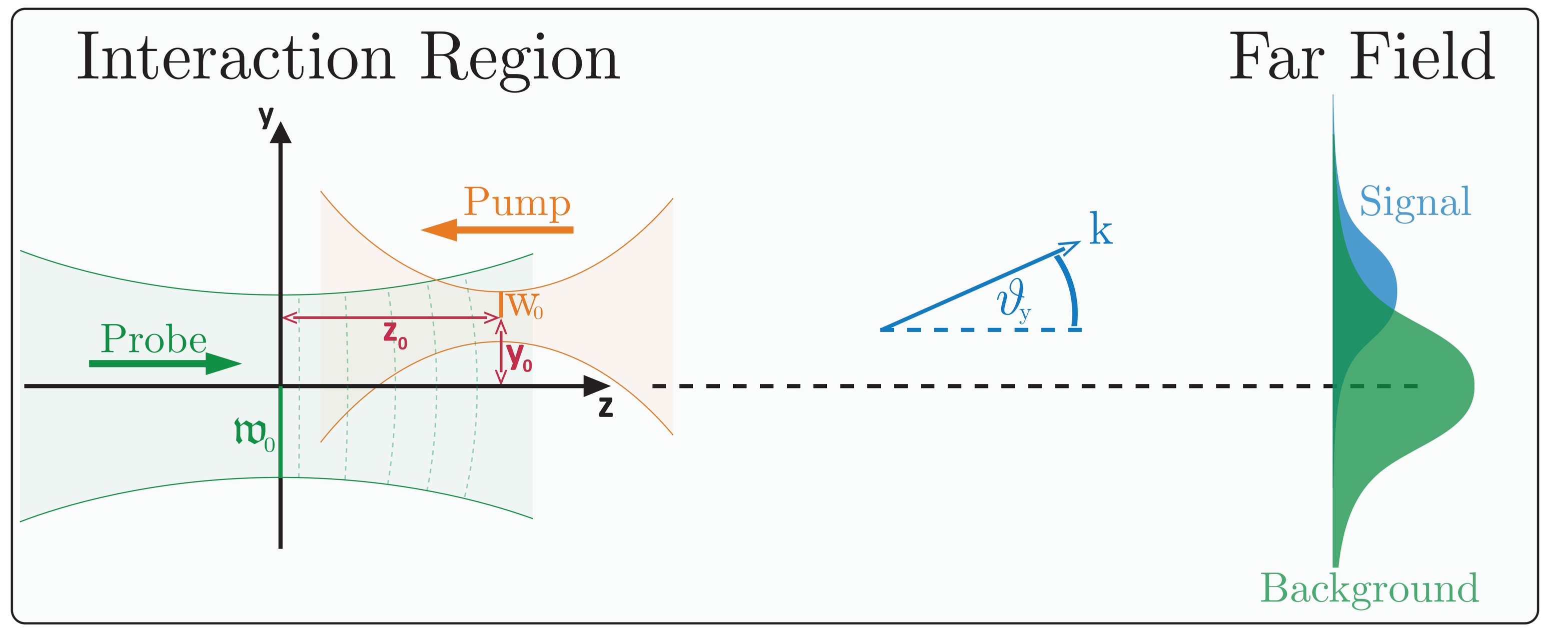

We assume a pump-probe-setup as promising experiment: a strong pump field (with field profile E) imprints certain properties on the quantum vacuum, which are to be probed by an additional field ($\mathfrak{E}$). Both pulses are chosen to be Gaussian:

$$\mathfrak{E}(x) = \mathfrak{E}_0\, \mathrm{e}^{-\left(\frac{z-t}{T/2}\right)^2}\frac{\mathfrak{w}_0}{\mathfrak{w}(z)}\mathrm{e}^{-\frac{x^2+y^2}{\mathfrak{w}^2(z)}}\cos\left(\omega(z-t)+\frac{\omega(x^2+y^2)}{2R(z)} - \arctan\left(\frac{z}{\mathfrak{z}_R}\right)\right) ,$$

The scattering matrix element then revolves around the Fourier integral:

$$S(\mathbf{k}) \propto \int \mathbf{d^4x}\, \mathfrak{E}(\mathbf{x})\, \mathbf{E}^2(\mathbf{x})\, \mathbf{e}^{\mathbf{ik(\hat{k}\cdot x - t)}}$$

Beams are counter-propagating with the probe focussed at the origin; the pump's may be set at finite offset x_0^μ.

- We studied two scenarios: A SACLA test parameter set (A), the other a possible future HIBEF one (B).
- z_0-Offsets were chosen in magnitude of the probe Rayleigh range $\mathcal{O}(\mathfrak{z}_R)$, y_0 of the probe waist $\mathfrak{w}_0$.
- Additionally the beam quality factor M^2 has been implemented into the probe pulse.

Setup:	A [1]	B
Probe Parameters:		
waist $\mathfrak{w}_0$ [μm]	6	3
pulse duration T [fs]	17	17, 220
frequency ω [keV]	9.8	12.914
pulse energy $\mathfrak{W}$ [mJ]	0.47	2.07
Pump Parameters:		
waist w_0 [μm]	9.8	1.0
pulse duration τ [fs]	40	40
Rayleigh range z_R [μm]	377.15	3.93
pulse energy W [J]	2.1×10^{-4}	12.5

3. Setup A: Benchmark Scenario

Recreation of previous results [1]: Far-field angular distribution of signal photons $\mathrm{d}^2N(\varphi,\vartheta)/(\mathrm{d}\varphi\,\mathrm{d}\cos\vartheta)$, obtained from numerical evaluation using Setup A parameters with two different focal offsets. These distributions are furthermore juxtaposed to the analogue density for an infinite Rayleigh range approximation (IRRA).

	Setup A	
Offset:	(a)	(b)
x_0 [μm]	0	0
y_0 [μm]	0	3.7
z_0 [m]	0.85	0.85

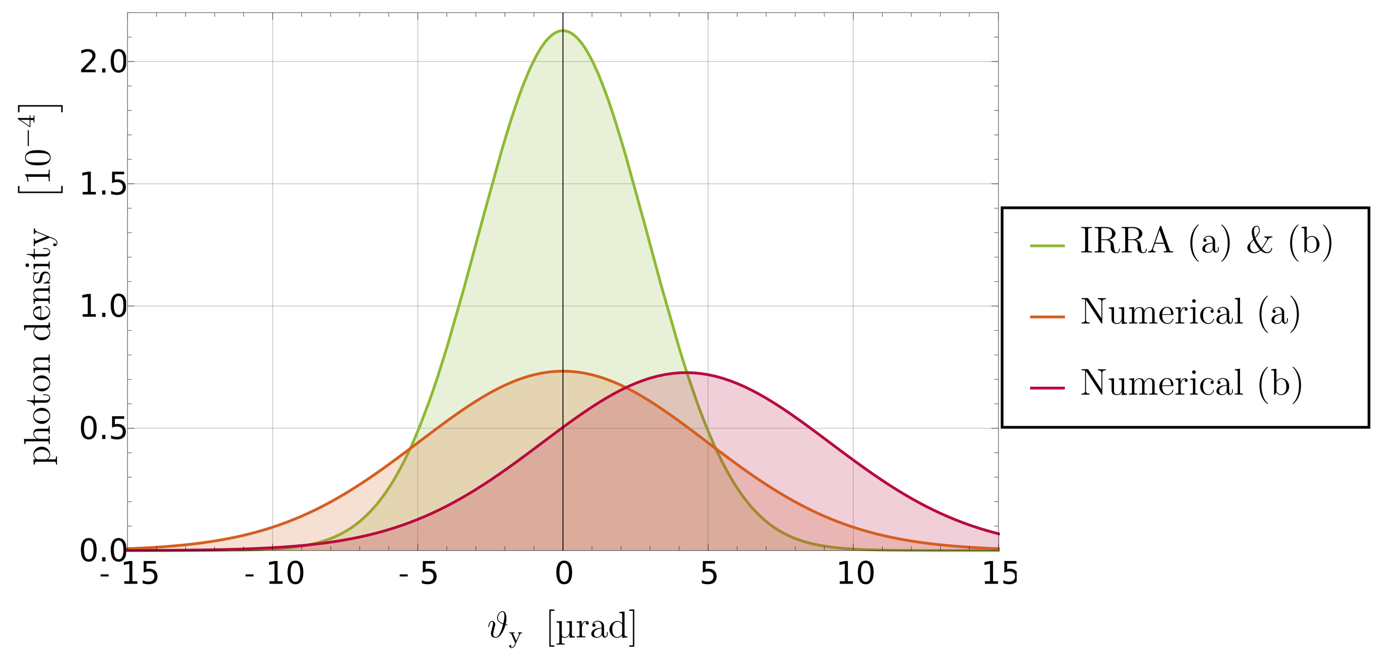

4. Setup B: Offset-Related Signal Distribution Properties

- Signal density can only be determined numerically. A local approximation however allows for analytical approximations of the angular shift $\Delta\vartheta_{\rm s,y}$ and signal divergence $\theta_{\rm s}$:

$$\Delta\vartheta_{\rm s,y} \simeq \frac{4M^2}{\omega\mathfrak{z}_R}\frac{z_0\, y_0}{2\mathfrak{w}(z_0)^2 + w_0^2} , \qquad \theta_{\rm s} \simeq \frac{2}{\omega\mathfrak{w}(z_0)}\sqrt{\frac{[1+2(\frac{\mathfrak{w}(z_0)}{w_0})^2]^2 + (\frac{z_0 M^2}{\mathfrak{z}_{\rm R}})^2}{1+2(\frac{\mathfrak{w}(z_0)}{w_0})^2}} ,$$

- For fixed $z_0 > 0$ these predict the angular offset to be linearly in and the divergence independent of y_0, which is confirmed by numerical evaluation below.
- The total expected number of signal photons $N_{\rm tot}$ undergoes exponential damping from any form of focal shift.

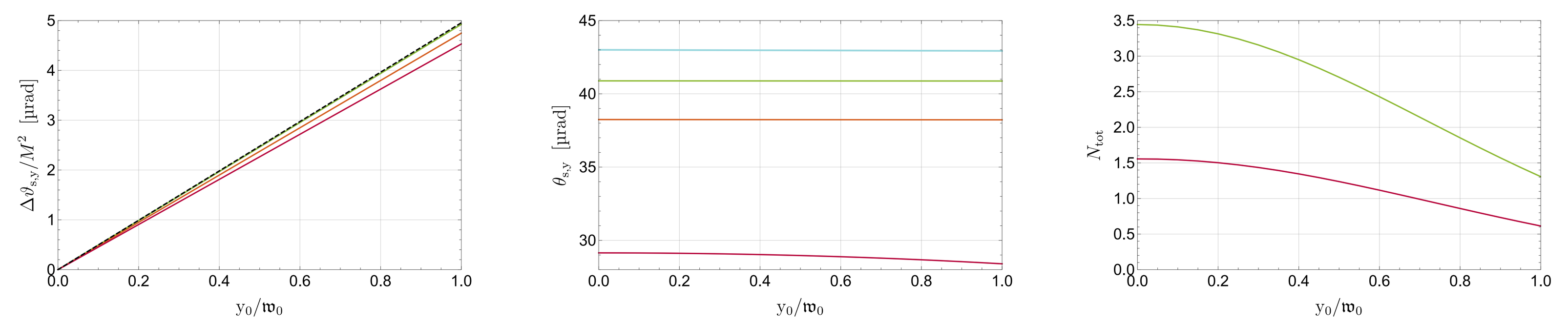

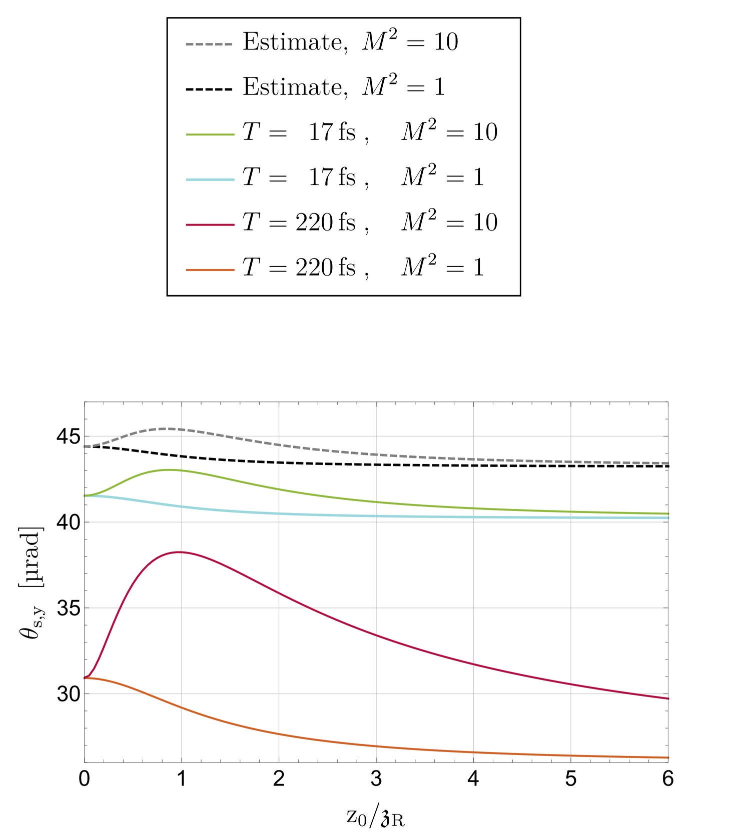

- Up to the threshold $M^2 \approx \sqrt{1+2\left(\frac{\mathfrak{w}_0}{w_0}\right)^2}$ $\theta_{\rm s}(z_0)$ monotonically decreases towards a lower boundary.
- For M^2 above this threshold a divergence peak develops. We assume this to be a mathematical artifact due to the Helmholtz equation not being obeyed for any $M^2 > 1$.
- Divergence $\theta_{\rm s,y}(z_0)$ shows qualitative agreement between numerical results and above estimate; deviations stem from the approximation being local.

5. Setup B: Prospective Experiment

Far-field distribution of B parameters shows region where signal surpasses background at $\vartheta_y \gtrsim 40$ μrad. Combined focal yz-offset generates an angular scattering assymetry affecting the respective gains. An increased probe pulse duration additionally dampens and narrows the signal.

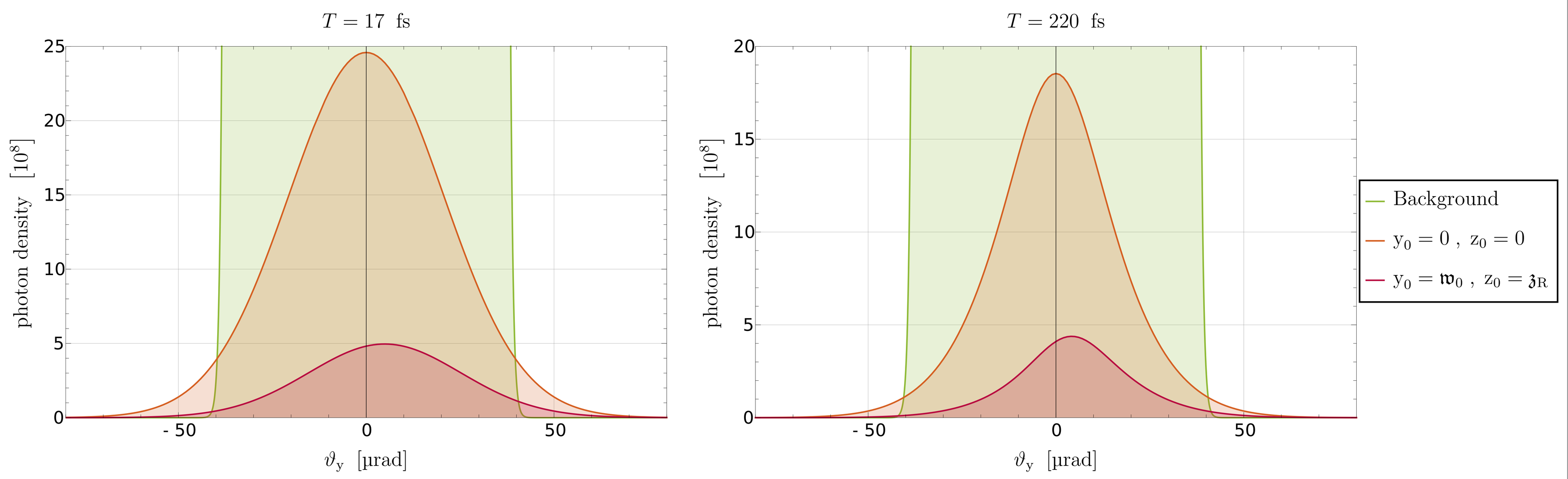

Table shows the expected full gain $N_{\rm tot}$, angular intersection points with background $|\vartheta_{\rm y,L/R}|$ and respective gains beyond these points, as well as the corresponding signal distribution assymetry.

T [fs]	z_0 [m]	y_0 [μm]	$N_{\rm tot}$	$\lvert\vartheta_{\rm y,L}\rvert$ [μrad]	$N_{\rm tot,L}$	$\lvert\vartheta_{\rm y,R}\rvert$ [μrad]	$N_{\rm tot,R}$	$\frac{N_{\rm tot,R}+\mathfrak{N}_{\rm R}}{N_{\rm tot,L}+\mathfrak{N}_{\rm L}}$
17	0	0	6.68	39.69	0.19	39.69	0.19	1
	0.29	0	3.44	40.17	0.089	40.17	0.089	1.00
	0.29	3.0	1.31	41.18	0.030	40.53	0.032	0.92
220	0	0	2.95	40.53	0.044	40.53	0.044	1
	0.29	0	1.56	41.01	0.020	41.01	0.020	1.00
	0.29	3.0	0.61	42.06	0.0067	41.31	0.0073	0.89

Conclusion and outlook

- Precise simulation of probe-pump collisions of Gaussian beams with focal offsets, recreating previous results [1].
- We studied the influence of focal shifts on the resulting signal photon distribution:
- With increased focal shifts the angular distribution offset increases linearly, while total signal is exponentially damped.

- Further usage of signal-to-background separation by focal shifting. Otherwise an indicator on how imprecise shots affect signal gains.
- Measurement of distribution assymetry might prove useful.
- Setup expandable by choice of different beam profiles, e.g. Hermite modes, flattened Gaussian beams etc.

7. References

[1] Y. Seino, T. Inada, T. Yamazaki, T. Namba and S. Asai, *New estimation of the curvature effect for the X-ray vacuum diffraction induced by an intense laser field*, Prog. Theor. Exp. Phys. **2020**, 073C02 (2020), doi:10.1093/ptep/ptaa084.

Felix Karbstein and Ricardo R. Q. P. T. Oude Weernink,
X-ray vacuum diffraction at finite spatio-temporal offset,
arXiv:2107.09632 [hep-ph].

E-mail: R.OudeWeernink@gsi.de